Received: 23 August 2023 | Revised: 19 October 2023 | Accepted: 26 October 2023

DOI: 10.1096/fj.202301611R

RESEARCH ARTICLE

The FASEB Journal

Conserved and species-specific transcriptional responses to daily programmed resistance exercise in rat and mouse

Mark R. Viggars[1,2,3] | **Hazel Sutherland**[1] | **Christopher P. Cardozo**[4,5] | **Jonathan C. Jarvis**[1]

[1]Research Institute for Sport & Exercise Science, Liverpool John Moores University, Liverpool, UK

[2]Department of Physiology and Aging, University of Florida, Gainesville, Florida, USA

[3]Myology Institute, University of Florida, Gainesville, Florida, USA

[4]Spinal Cord Damage Research Center, James J. Peters VA Medical Center, Bronx, New York, USA

[5]Icahn School of Medicine, Mount Sinai, New York, New York, USA

Correspondence
Mark R. Viggars, Department of Physiology and Aging, University of Florida, Gainesville, FL, USA.
Email: m.viggars@ufl.edu

Jonathan C. Jarvis, School of Sport and Exercise Science, Liverpool John Moores University, Byrom Street, Liverpool L33AF, UK.
Email: j.c.jarvis@ljmu.ac.uk

Funding information
U.S. Department of Defense (DOD), Grant/Award Number: SC190031; U.S. Department of Veterans Affairs (VA), Grant/Award Number: I50RX002020

Abstract

Mice are often used in gain or loss of function studies to understand how genes regulate metabolism and adaptation to exercise in skeletal muscle. Once-daily resistance training with electrical nerve stimulation produces hypertrophy of the dorsiflexors in rat, but not in mouse. Using implantable pulse generators, we assessed the acute transcriptional response (1-h post-exercise) after 2, 10, and 20 days of training in free-living mice and rats using identical nerve stimulation paradigms. RNA sequencing revealed strong concordance in the timecourse of many transcriptional responses in the tibialis anterior muscles of both species including responses related to "stress responses/immediate-early genes, and "collagen homeostasis," "ribosomal subunits," "autophagy," and "focal adhesion." However, pathways associated with energy metabolism including "carbon metabolism," "oxidative phosphorylation," "mitochondrial translation," "propanoate metabolism," and "valine, leucine, and isoleucine degradation" were oppositely regulated between species. These pathways were suppressed in the rat but upregulated in the mouse. Our transcriptional analysis suggests that although many pathways associated with growth show remarkable similarities between species, the absence of an actual growth response in the mouse may be because the mouse prioritizes energy metabolism, specifically the replenishment of fuel stores and intermediate metabolites.

KEYWORDS

exercise, functional electrical stimulation, metabolism, muscle atrophy, muscle hypertrophy, transcription

1 | INTRODUCTION

Muscle strength has been identified as a predictor of all-cause mortality, so interventions that improve or ameliorate the deterioration of muscle strength with age or disease are important preventative and interventional aspects of medicine.[1,2] Indeed, resistance exercise training has been shown to be beneficial in promoting health in a

Abbreviations: BP, biological process; CPN, common peroneal nerve; DAVID, Database for Annotation, Visualization and Integrated Discovery; DEG, differentially expressed gene; FDR, false discovery rate; GO, gene ontology; HOMER, Hypergeometric Optimization of Motif EnRichment; Hz, Hertz, (impulses per second); IPG, implanted pulse generator; KEGG, Kyoto encyclopaedia of genes and genomes; min, minute; NADH, nicotinamide adenine dinucleotide; QA/QC, quality assurance/quality control; reps, repetitions; TA, tibialis anterior.

variety of disease states including aging, metabolic disorders, cardiovascular disease, cancer cachexia, and neurological conditions.[3–6]

Resistance exercise causes metabolic and mechanical perturbations in the muscle that initiate acute signaling cascades,[7–11] with both local and systemic effects.[12] With regular resistance training, these transcriptional changes can lead to increases in muscle size, quality, strength, and improvements in metabolic function, but the molecular underpinnings of such adaptations are only partially understood.

Mice remain in many cases the most desirable model for research into the molecular biology underpinning the benefits of exercise because the mouse genome is well annotated, and because tools exist for relatively easy and precise manipulation of the genome so that gene function can be investigated by gain or loss of function studies with global or tissue-specific techniques.[13] Adaptation to endurance exercise can be easily studied in rodents through voluntary or forced wheel/treadmill running, but interventions that mimic resistance-like exercise are more challenging to set up.[14] An established method to mimic the "sets and reps" style of resistance-like exercise is the use of high-frequency contractions delivered to the hindlimb via electrical stimulation of the sciatic nerve so that contractions of the ankle dorsiflexors are resisted by simultaneous contractions of the plantarflexors. In the rat, this results in extensive hypertrophy of the dorsiflexors (10%–30%) in a matter of weeks,[15–19] without extensive damage or regeneration. In recent years, we have developed this co-contraction technique by means of implantable stimulators for use in free-living rats and mice so that anesthesia during stimulation is not required. Similar exercise paradigms in the mouse seem to be protective against muscle wasting,[20,21] but to the best of our knowledge result in little or no muscle growth[22] and we confirm that finding here over a period of 3 weeks of daily training. Several papers on the other hand have used the co-contraction paradigm to interrogate the signaling response to high-force contractions in mice.[11,23,24]

There are a number of potential molecular factors that may determine these differences in muscle growth between species, including but not limited to the basal transcriptional, epigenetic, and metabolic properties of the hindlimb muscles that dictate the responsiveness to exercise and protein turnover rates.

Here, we focus on the transcriptional differences that are associated with the lack of increase in muscle mass in mouse dorsiflexors. We used RNA sequencing to compare the acute transcriptional responses to resistance exercise as the training status changes over a period of 3 weeks of daily training in mice and rats. Uniquely, our resistance exercise paradigm allows identical nerve stimulation patterns to be delivered by implantable pulse generators in free-living mice and rats providing a highly controlled contraction paradigm. Our transcriptome analysis highlights both concordant or conserved and discordant or species-specific transcriptional responses to the identical nerve-stimulated resistance exercise over a period of daily training which may underpin the differences in growth response.

2 | MATERIALS AND METHODS

2.1 | Experimental design

The animal experiments were conducted under the provisions of the Animals (Scientific Procedures) Act 1986 and approved by the British Home Office (PA6930221). Male C57BL/6J mice were originally purchased from Charles River UK Limited and were kept on a 12:12 light:dark cycle. Mice were group housed with 3–5 per cage and kept in their pre-operative social groups post-implantation. Pulse generators were surgically implanted at ~5 months of age for both mice and rats. Details of the Wistar rats used in this analysis which was previously published but reanalyzed are available here[17] and in the "Bioinformatic Analysis" section of the methods.

2.2 | Resistance training protocol and pattern

Animals received 1 session per day of SpillOver resistance training in the left hindlimb via stimulation from an implanted pulse generator (IPG) as previously described,[17–19,25] for 2 ($n = 2$), 10 ($n = 3$), or 20 days ($n = 3$). The training was conducted between ZT1-4, where ZT0 indicates lights on and ZT12 indicates lights off. The dorsiflexor muscles received supramaximal activation via a cathode placed underneath the common peroneal nerve, while the anode was positioned underneath the tibial nerve and stimulated the plantarflexor muscles with the stimulus current adjusted during the implant operation to provide enough recruitment to provide resistance against the contraction of the dorsiflexors so that the dorsiflexors contracted isometrically or with slightly eccentric contractions for the duration of the study.

Daily training was delivered automatically by the IPG and consisted of an initial 10 seconds of preparatory stimulation at a low frequency (F = 4 Hz, phase width = 258 μs, current = approximately 1 mA), followed by 5 sets of 10 tetanic contractions at 100 Hz. Each contraction lasted for 2 s with 2 s of rest between contractions and 2.5 min of rest between sets. Stimulation was delivered only in the left

hindlimb. Muscles of the right hind-limb acted as unstimulated contralateral controls.

2.3 | Implantable pulse generators

Silicone encapsulated radio frequency controlled implantable pulse generators (IPGs) (MiniVStim 12B, Competence Team for Implanted Devices, Center for Medical Physics and Biomedical Engineering, Medical University) were used to deliver electrical impulses which invoke contraction of the targeted nerves/muscles.

Pulse generators were programmed wirelessly via an external programming device and an Android-driven tablet computer (Xperia Tablet Z, Sony Corporation) as previously described.[17] This allowed for fine adjustment of the stimulation amplitude individually for each animal. After initial setup, the customized stimulation pattern was saved to the implant, enabling automatic daily delivery of SpillOver stimulation to the targeted nerves. The electronic circuit was connected for use in rats to a 1/3N lithium battery. In mice, the same circuit was driven by a 1220 lithium battery to reduce the overall size of the implant.

2.4 | Surgical procedure

Animals were anesthetized during implant procedures by inhalation of a gaseous mixture of isoflurane in oxygen at approximately 3% for induction and 1%–2% for maintenance. Once anesthetized, a subcutaneous injection of Enrofloxacin for antibiotic cover (5 mg/kg body mass (Baytril®) and an intramuscular injection of Buprenorphine for analgesia at 0.05 mg/kg body mass in rat and 0.1 mg/kg body mass in mouse (Temgesic, Indivior) into the right quadriceps were given. Strict asepsis was maintained throughout the procedure. In rats, the IPGs were implanted into the abdominal cavity accessed by a lateral incision through the skin and peritoneum, between the rib cage and pelvis on the left side of the animal. A polyester mesh attached to the IPG was incorporated into the suture line closing the peritoneum, securing the device against the abdominal wall. In the mouse, the implant was placed subcutaneously on the flank. Two PVC-insulated stainless-steel electrode leads (Cooner Sales Company) with terminal conductive loops were fed from the implant site and tunneled under the skin to the lateral side of the left hindlimb, just above the knee. A second incision was made through the skin and biceps femoris muscle to give access to the common peroneal nerve (CPN) under which the cathode was placed (to stimulate the dorsiflexors). The anode was placed in the muscular tissue deep to the tibial nerve about 5 mm distal to its bifurcation from the sciatic nerve to allow SpillOver stimulation to produce additional partial activation of the plantarflexors and thus to resist the contraction of the dorsiflexors. All incisions were closed in layers and 7 days were allowed for recovery from surgery before the start of the training protocol which lasted for 2, 10, or 20 days. The surgery was well-tolerated by all mice, losing only $2.3 \pm 3.36\%$ of body weight from pre-surgery to 7-day recovery post-surgery.

2.5 | Histological analysis

Fiber cross-sectional area labeling for dystrophin, NADH activity, and hematoxylin and eosin staining and subsequent analysis was performed as previously described.[17,19,25–27] Mouse tibialis anterior samples were sectioned at 10 µm using an OTF5000 Cryostat (Bright Instruments) onto Thermo Scientific SuperFrost Plus Adhesion slides (Thermo Fisher Scientific Inc.). Muscle cross sections were labeled with a polyclonal dystrophin antibody (Cat. No. PA5-32388; Thermo Fisher Scientific) at (1:200) and appropriate fluorescently conjugated anti-rabbit IgG (H + L) secondary with Alexa Fluor 488 (1:500) was used to demarcate the inside of the sarcolemma.

Once labeled, whole muscle cross sections were imaged using a Zeiss LSM 900 confocal with a ×20 objective for fluorescence and a Leica LMD6 microscope with a ×10 objective for brightfield imaging. Multiple images were automatically stitched together using the tilescan feature in the Zen Blue v 3.8 system for fluorescence and the Leica Application Suite for brightfield. Images were automatically processed for fiber cross-sectional analysis using MyoVision 2.0 software using default parameters for mouse.[25]

2.6 | Muscle sampling, RNA isolation, and RNA library preparation and sequencing

Animals were euthanized using a rising concentration of carbon dioxide, followed by cervical dislocation. Tibialis anterior (TA) muscles from both hind limbs were immediately harvested, cleaned of excess connective tissue, and weighed. A small cross-sectional sample was frozen in isopentane above liquid nitrogen for histology and the remainder flash frozen in liquid nitrogen for subsequent RNA extraction. About 30 mg of mouse TA muscle was added to MagNA Lyser Green Bead tubes (Roche 03358941001) with 600 µL lysis buffer (PureLink RNA Mini Kit, Invitrogen 12183018A) and homogenized using a MagNA Lyser (Roche) at 6500 rpm for three, 40-s sets with cooling in a rotor block at −20°C in between.

Homogenates were centrifuged at 12 000**g** for 10 min. The supernatant (400 μL) was mixed with 400 μL ethanol and added to a spin cartridge (PureLink RNA Mini Kit). RNA was bound to the column by centrifugation and was washed multiple times per the manufacturer's recommendations. RNA was eluted in nuclease-free water from the column. RNA integrity numbers (RIN) were determined on an Agilent TapeStation 2200 (Agilent). All samples prepared for sequencing had RIN values of at least 8. Libraries were created using Poly-A tail selection using the Illumina mRNA Prep kit (Illumina, Inc.) kit and pooled to equal molarities and sequenced on the Novaseq 6000 (Illumina, Inc.) S4 2 × 150 bp platform by the University of Florida Interdisciplinary Centre for Biotechnology Research (ICBR), RRID:SCR_019145 and SCR_019152. For mouse tissue RNA sequencing, the contralateral unstimulated limbs ($n = 8$) were used, alongside ($n = 2$) for 2 days of training and ($n = 3$) for 10 and 20 days of training. RNA sequencing from the rat experiments was taken from the GEO accession GSE196147 but realigned to the latest genome annotation model as described below. The RNA extraction and sequencing from the rat tissue has been described previously.[17]

2.7 | Bioinformatic Analysis, HOMER motif analysis and CIBERSORTx digital cytometry for single-cell deconvolution of bulk RNA sequencing

FastQ files were imported to Partek® Flow® Genomic Analysis Software Partek Inc.) for pipeline processing. Pre-alignment QA/QC was performed on all reads prior to read trimming below a Phred quality score of 25 and adapter trimming. STAR alignment 4.4.1d was used to align reads to the *Rattus norvegicus*, Rn7 genome assembly or the *Mus musculus*, mm10 genome assembly.[28] The data generated for the rat has previously been published with analysis and alignment performed on the earlier Rn6 genome assembly. Rn7 has significant improvements from Rn6 including increased genome coverage and reduced gaps between scaffolds making it comparable in quality to the current human and mice genome assemblies.[29,30] Aligned reads were quantified to Ensembl annotation models and gene expression normalized using DESeq2 median of ratios[31] and DEGs identified through the Partek® Flow® DESeq2's binomial generalized linear model with Wald testing for significance between conditions set at an FDR of 5%. QA/QC data and normalized count information is available in Data S1.

Filtered lists for common and species-specific differentially expressed genes (DEGs) were extracted and imported to DAVID. DAVID functional annotation was performed using a high-stringency cut-off for pathways associated with the KEGG pathway database, the Reactome pathway database and the Gene Ontology (GO) biological process, and cellular component databases.[32] A background list was used for each DAVID analysis as found in Figure 2H for each species. Data contained in individual gene plots was generated by Log^2 transforming the *Z*-scores of normalized Deseq2 counts.

HOMER (v4.11) motif analysis was performed on DEGSs, to identify enrichment of known motifs (6–12 bp long) in the gene body and up to 2 kb upstream of the transcription start site, results from which can be found in Data S1.

Single-cell deconvolution was performed on Deseq2 normalized mouse and rat data using a digital cytometry and machine learning platform, CIBERSORTx.[33] Using an established single cell dataset[34] as a background signature matrix file, we imputed cell fractions using default settings. We compared the relative cellular fractions in stimulated and unstimulated mouse and rat muscles using one-way ANOVA analysis as described below.

FIGURE 1 Experimental model and timecourse of changes in muscle mass with identical daily stimulation patterns in the rat and mouse. (A) Schematic of pulse generator surgical implantation and electrode placement. The cathode was placed underneath the common peroneal nerve, controlling motor activity in the dorsiflexors. The anode was placed underneath the tibial nerve, controlling motor activity in the plantarflexors. The "SpillOver" stimulation paradigm allows for partial activation of the larger plantarflexor muscle group, providing a resisted contraction in the dorsiflexors. (B) Percent changes in muscle mass (mg) per body mass (g) over time in response to daily training between stimulated limbs and unstimulated contralateral controls (mean ± SD). (C) Representative dystrophin immunofluorescent labeling of a 10-day stimulated mouse muscle and unstimulated contralateral control. (D) Representative hematoxylin and eosin stain from 10-day stimulated muscle and unstimulated contralateral control muscle. (E) Representative NADH tetrazolium reductase staining from 10-day stimulated muscle and unstimulated contralateral control muscle. Scale bars indicate 2000 μm/2 mm for whole cross-sections and 100 μm for regions of interest. (F) Fiber cross-sectional area μm^2 measurements from whole cross-sections of mouse tibialis anterior assessed automatically using MyoVision 2.0. (G) Percent changes in muscle cross-sectional area in μm^2 between unstimulated muscles in the right leg and stimulated muscle in the left leg. (H) Percent changes in NADH grayscale intensity between unstimulated muscles in the right leg and stimulated muscle in the left leg. Corresponding symbols to highlight statistical significance are as follows: *$p \leq .05$, **$p \leq .01$, ***$p \leq .001$, and ****$p \leq .0001$.

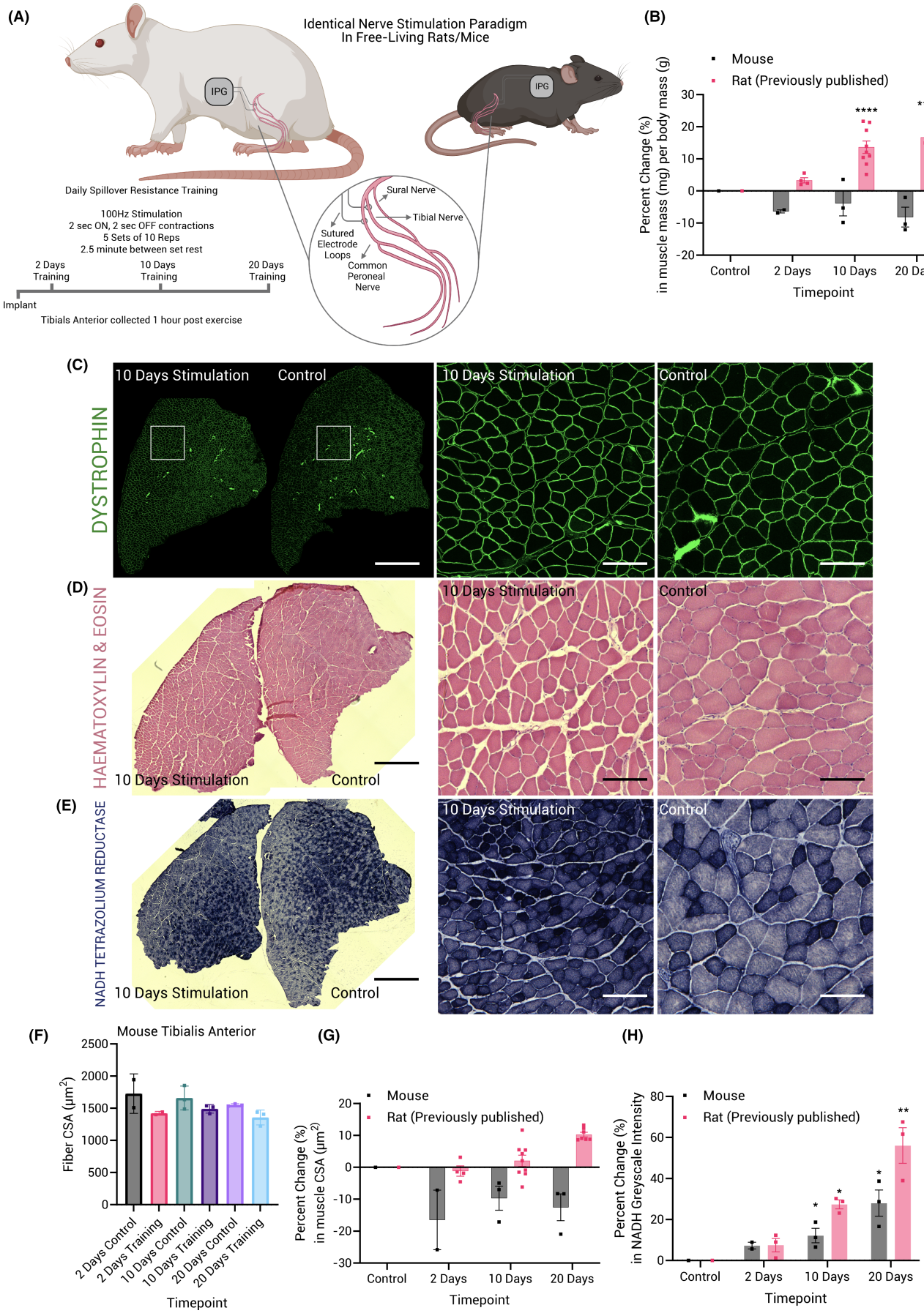

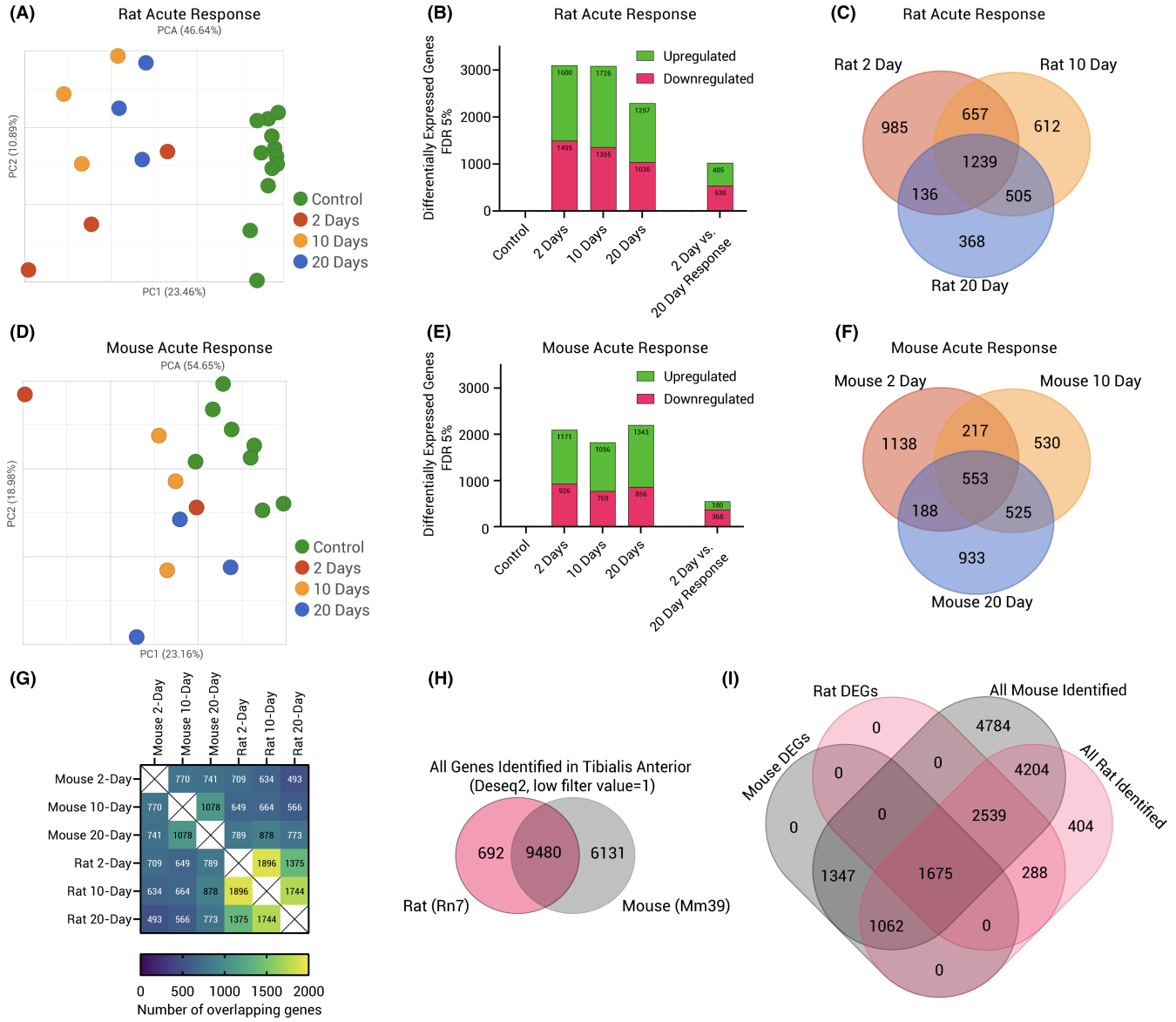

FIGURE 2 Summary of the transcriptional response across species in response to acute resistance exercise. (A) RNA sequencing principal components analysis of the rat acute exercise response in relation to training status. (B) Differentially expressed genes relative to control in response to exercise in the rat using a false discovery rate of 5%. (C) Venn diagram analysis of training status-specific responses to acute exercise in the rat. (D) RNA sequencing principal component analysis of the mouse acute exercise response in relation to training status. (E) Differentially expressed genes relative to control in response to exercise in the mouse using a false discovery rate of 5%. (F) Venn diagram analysis of training status-specific responses to acute exercise in the mouse. (G) Heatmap of differentially expressed genes overlapping between species and stages of training. (H) Venn diagram analysis summarizing the number of total genes identified from mouse (Mm39) and rat (Rn7) tibialis anterior muscles using the Deseq2 low filter value which removes genes with a mean low filter value of 1 or less. (I) Venn diagram analysis overlapping the number of total differentially expressed genes in rat and mouse, as well as the number of genes identified in rat and mouse tissue. Data for C, F, H, and I are available in Data S2.

2.8 | Statistical information

Muscle mass data are presented as the % change between the left experimental hind-limb and right internal contralateral control hind-limb for normalized muscle mass (mg/kg bodyweight). The resultant percentage changes were then compared via one-way ANOVA, followed by Tukey's post-hoc analysis to confirm differences between groups in GraphPad Prism 9.0 software. All data are presented as mean ± SD. The threshold for statistical significance was taken at $p < .05$. Corresponding symbols to indicate statistical significance are as follows: *$p \leq .05$, **$p \leq .01$, ***$p \leq .001$, and ****$p \leq .0001$. Pearson's correlations were also performed in GraphPad Prism 9.0 software. Individual gene plots are presented as Log^2 Z-scores of normalized Deseq2 counts.

2.9 | Ethics statements

This study received funding from DOD SCIRP IIR SC190031 (to CPC and JCJ), VA Rehabilitation Research and Development Service I50RX002020. The views represented in this manuscript are not reflective of the United States Government or the Department of Veterans Affairs.

3 | RESULTS

3.1 | The timecourse of changes in muscle mass following identical activity/loading patterns in mice and rats

Daily SpillOver resistance training in rats results in a progressive increase in muscle mass after 2 (4.2 ± 3.3%, $p = .37$), 10 (13.1 ± 5.2%, $p < .0001$), and 20 days of consecutive resistance exercise (16.1 ± 4.2%, $p < .0001$) compared with sham surgery (−0.9 ± 1.4%), as previously reported in a separate study.[19] The increase in muscle mass plateaus between 10 and 20 days of training ($p = .23$), (Figure 1B). Similar experimental paradigms in other laboratories have yielded similar results in the rat.[15,35] Interestingly, the same nerve stimulation paradigm in mice has anecdotally been reported not to result in a hypertrophic response. In our mouse experiments, we observed small yet insignificant reductions in muscle mass after 2 (−6.4 ± 0.5%), 10 (−3.8 ± 5.6%), and 20 days (−8.1 ± 4.4%) of training respectively despite using the identical nerve stimulation paradigm as used in the rats (Figure 1B). Through immunofluorescent dystrophin labeling of cross-sections (Figure 1C), we were able to identify fiber outlines and identify average cross-sectional area of all fibers using MyoVision 2.0. No significant differences were found between groups as the experiment was likely underpowered to find significant differences, although trends were clear when muscle cross-sectional area was plotted as a percent change between the left stimulated tibialis anterior muscle and right unstimulated contralateral control (Figure 1F,G). This loss in muscle mass and fiber-cross-sectional area occurred without histological evidence of denervation, damage, or degeneration as evidenced in Figure 1D by the absence of excess connective tissue, round fibers, or central nuclei. We also observed little to no differences in the gene expression of *Myh3* and *Myh8* which encode embryonic and neonatal myosins respectively in mice and rats, Data S1. This suggests that there are similarities in whatever small damage response is generated following stimulation. NADH tetrazolium reductase staining, which is used as a proxy marker for mitochondrial content or oxidative capacity showed progressive significant increases with 2 (7.2 ± 1.6%), 10 (12.2 ± 5%), and 20 days (28 ± 9.1%) of daily training in the mouse as depicted in Figure 1E,H. These changes were similar in direction, but the magnitude of change was lower in the mouse compared to our previously published data using the same stimulation paradigm in rat.

3.2 | Timecourse assessment of transcriptional responses to identical daily stimulation patterns in the rat and mouse

To understand the potentially divergent mechanisms resulting in substantial growth in stimulated rat muscle, but lack of hypertrophy in the mouse, we performed RNA sequencing on the TA muscles from the mice. These responses were compared to an existing dataset in the rat, but the rat data was newly realigned to the latest rat genome assembly (Rn7). Rn7 has significant advantages over the previous Rn6 release of the rat genome as previously discussed,[29,30] which justify a new investigation of the rat dataset and allow a more appropriate comparison with transcripts from the mouse genome.

Our principal components analysis showed a clear distinction in both mice and rats between control and the acute exercise response at different levels of training status (Figure 2A,D). Using a 5% FDR cut off to identify significant DEGs versus the group of contralateral control muscles, we identified 3095, 3081, and 2293 genes in the acute response to exercise after 2, 10, and 20 days of training respectively in the rat, (Figure 2B). The number of overlapping genes between the 2- and 20-day response was 1023 genes, indicating that the acute exercise response changes significantly during a period of daily training in the rat. This is further highlighted in Figure 2C, where we show that only 1239 out of 4502 genes (27.5%) were always differentially expressed at each timepoint, and thus independently of training status.

The total number of DEGs in the mouse in response to acute resistance exercise was about two-thirds of the rat transcriptional response, even though the total number of genes identified in the transcriptome was greater for mouse than rat. Using the same statistical parameters as for the rat analysis to identify significant DEGs versus control muscles, we identified 2097, 1825, and 2199 genes in the acute response to exercise after 2, 10, and 20 days of training in the mouse (Figure 2E). The number of overlapping genes between the 2- and 20-day response was 548 genes and only 553 genes (13.5%) were consistently differentially expressed independently of training status (Figure 2F), showing the common phenomenon between species that the acute transcriptional response changed considerably as daily training progressed. Mouse DEGs and rat DEGs at each training status were compared and

the number of overlapping features is presented in a heatmap (Figure 2G). A similar number of genes at each training status were found to be common between species, 709, 664, and 773 after 2, 10, and 20 days of training. Because there are known differences in genome annotation between species, we further probed our datasets to investigate whether the total number of genes expressed in the TA muscle (control or any stage of training) in the mouse and rat differed and how much of the basal transcriptome was conserved (using Deseq2 low filter value of <1). Interestingly, there were 692 genes only expressed in the rat TA (4.2%) and 6131 specific to the mouse (37.6%), but 9480 (58.2%) which were expressed in both species (Figure 2H). Overall, 15 611 genes were identified in the mouse using this filter and 10 172 in the rat.

To investigate whether the differences in the total number of identified genes influenced the number of DEGs between species we performed a Venn diagram analysis of the total number of mouse DEGs, the total number of rat DEGs and the total number of identified genes in mouse and rat (Figure 2I). Of the total number of genes identified (16 303), 404 (2.5%) were only identified in the rat but not differentially expressed with training, 4784 (29.3%) were only identified in the mouse but not differentially expressed with training and 4204 (25.8%) were expressed in both species but not differentially expressed in response to acute resistance exercise in one or both species. In total, 288 genes (1.8%) were only identified in the rat and were differentially expressed. Conversely, 1347 (8.3%) of genes were only identified in the mouse and were also differentially expressed. Investigation of these genes revealed that most of them had no common ortholog in the other species, the gene had uncertain function, or they had uncharacterized locations within the genome assembly. A larger percentage of these were as expected found only in the mouse, suggesting that many rat orthologs are yet to be identified in the genome assembly. For these reasons, we chose genes identified in tibialis anterior muscles of both species for further investigation. Of genes identified in both species, 1062 (6.5%) were only differentially expressed in the mouse, 2539 (15.6%) were only differentially expressed in the rat and 1675 (10.3%) were differentially expressed in both species.

3.3 | Common training status-specific transcriptional responses to resistance exercise in the rat and mouse

To identify potential differences that might explain the different growth responses between species, we overlapped the DEGs at each training time point between species to identify common and species-specific elements changing in the transcriptome.

In the 2-day acute exercise response, only 709 (16.1%) of the total number of DEGs in rats and mice were found to be common between species (Figure 3A). Pearson's correlation of the Log^2 fold changes in the common DEGs revealed a significant positive correlation between species ($R = .71$, $p < .0001$) (Figure 3B). Analysis of these common and largely correlated features revealed enrichment of pathways related to stress responses, AMPK signaling, immune responses, autophagy, protein processing in the endoplasmic reticulum, glycogen metabolism, protein metabolism, and various processes involved directly or upstream of ribosome regulation and FoxO signaling pathways (Figure 3C).

In the 10-day acute exercise response, 664 genes (15.9%) were commonly differentially expressed between species (Figure 3D) and they showed a similar significant correlation ($R = .63$, $p < .0001$), (Figure 3E). However, pathway analysis revealed enrichment of a different set of pathways than in the 2-day acute exercise response. These included processes related to the extracellular matrix and collagen regulation, focal adhesion, proteoglycans, and PI3k-Akt signaling pathways (Figure 3F).

Again, the 20-day acute exercise response showed a similar percentage of DEGs common to both species (773, 21%) as previously noted with the 2- and 10-day responses. A similar significant positive correlation was identified in this gene set between species ($R = .66$, $p < .0001$). A number of enriched pathways shared similarities to the 2- and 10-day responses, but hemostasis, platelet activation, signaling, and aggregation pathways were specifically enriched at the 20-day timepoint. Many of the genes contained in these pathways are closely related to extracellular matrix and integrin remodeling.

We next investigated the genes involved in each identified pathway that showed common responses between species, plotting their Log^2 Z-scores in response to acute exercise across the training timecourse. Genes involved in the stress response, including genes classified as immediate-early genes that are transiently activated by a wide variety of cellular stimuli, showed strikingly concordant changes in expression in response to acute resistance exercise across this timecourse and thus with similar training status (Figure 4). Most of these genes are increased to their highest level in the 2-day exercise response with a gradual decline as training status increases. This pathway includes a number of transcription factors (*Ankrd1*, *Atf3*, *Csrnp1*, *Egr1*, *Fos*, *Hif1a*, *Jun*, *Junb*, *Jund*, *Myc*, *Nfatc3*), transcription co-activators (*Ppargc1a*), insulin-Akt-AMPK regulators (*Irs2*, *Mapk9*), nuclear receptors (*Nr4a1*, *Nr4a2*, *Nr4a3*), and heat shock factors (*Hspa1a*, *Hspa1b*, *Hspb1*, *Hspb2*, *Hspb6*, *Hspb7*, *Hspb8*) that have been shown to be upregulated specifically in myonuclei and are known to regulate a wide array of biological processes including

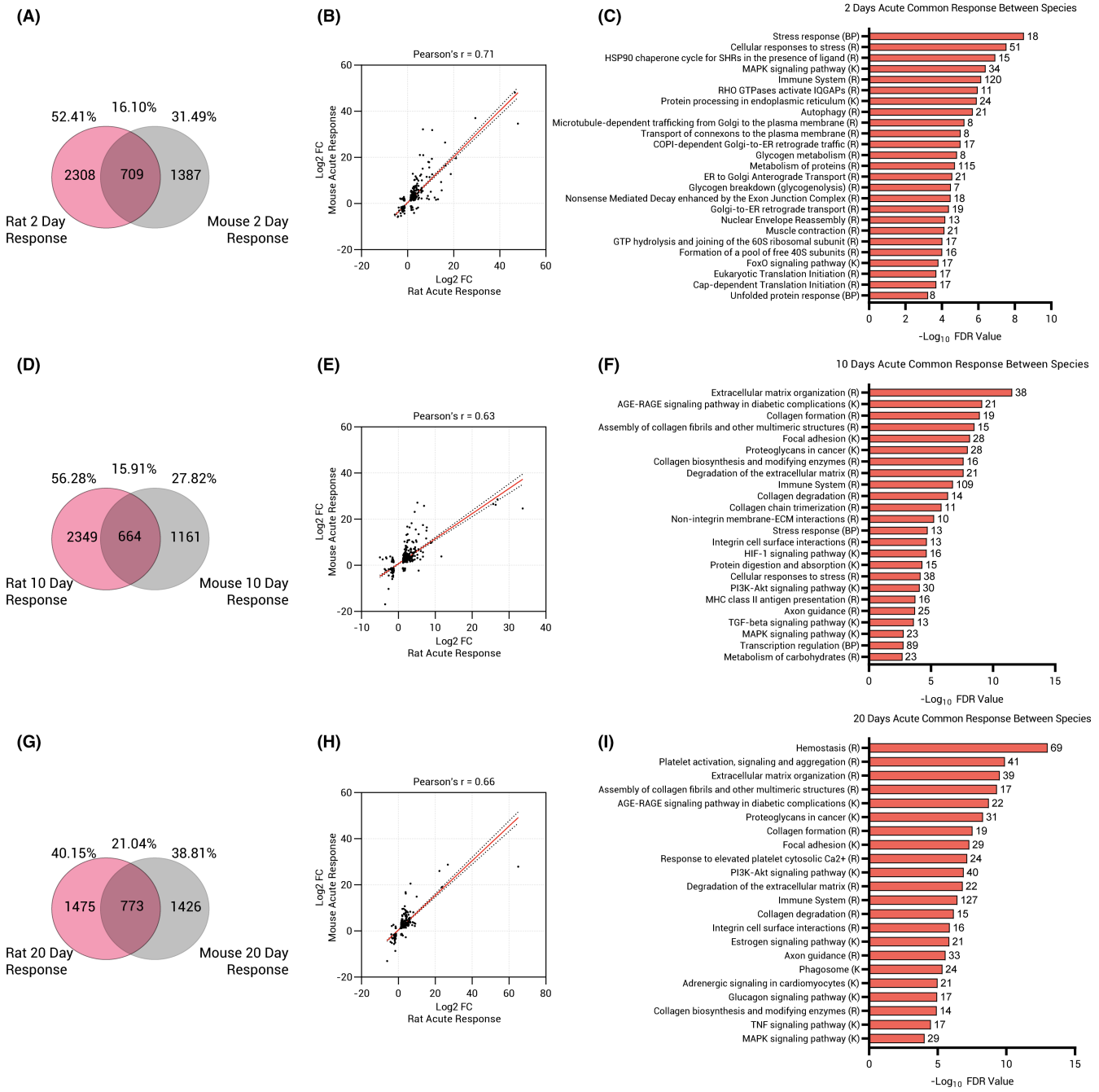

FIGURE 3 Common training status-specific acute transcriptional responses to resistance exercise in rats and mice. (A) Venn diagram analysis of differentially expressed genes (5% false discovery rate) in response to acute exercise between mouse and rat after 2 days of training. (B) Pearson's correlation (Log^2 FC normalized) of the 2-day acute exercise response of the shared differentially expressed genes identified in (A) Venn diagram. (C) Pathway analysis of the shared features identified in (A). (D) Venn diagram analysis of differentially expressed genes (5% false discovery rate) in response to acute exercise in mouse and rat after 10 days of training. (E) Pearson's correlation (Log^2 FC normalized) of the 10-day acute exercise response of the shared differentially expressed genes identified in (D) Venn diagram. (F) Pathway analysis of the shared features identified in (D). (G) Venn diagram analysis of differentially expressed genes (5% false discovery rate) in response to acute exercise between mouse and rat after 20 days of training. (H) Pearson's correlation (Log^2 FC normalized) of the 20-day acute exercise response of the shared differentially expressed genes identified in (G) Venn diagram. (I) Pathway analysis of the shared features identified in (G). Pathways and their associated databases are annotated as follows: KEGG pathway (K), reactome pathway (R), and GO biological process (BP). The number of genes associated with each pathway is presented adjacent to each pathway. Data for (A–I) are available in Data S2.

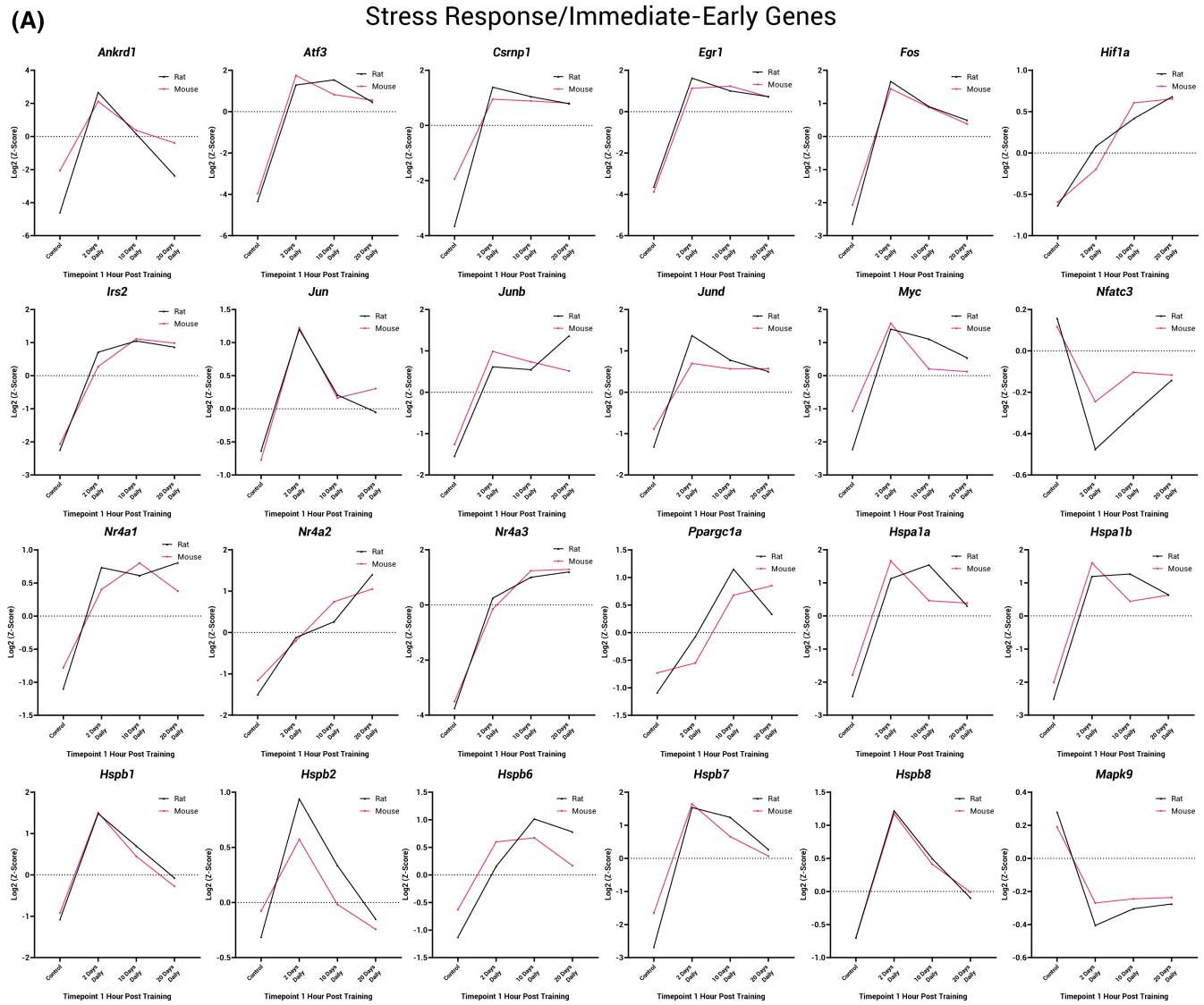

FIGURE 4 The timecourses for expression of stress response and "immediate early genes" show strong similarities between species in response to resistance exercise. (A) Log^2 *z*-scores of the Deseq2 normalized transcript abundance in control muscle and muscle after acute exercise with 2, 10, and 20 days of training history. Rat gene responses are indicated by a black line and mouse gene expression levels are indicated by pink lines.

metabolism and growth (Figure 4A). Many of these transcription factors including *Myc* and *Jun* also displayed similar temporal patterns in our HOMER motif analysis on the putative upstream regulators of differentially expressed genes.

Similarly, a large number of collagen and extracellular matrix-associated genes show notable concordance between species and with training status including genes encoding enzymes involved in collagen cleavage, synthesis, and maturation (*Adamsts2*, *Ctss*, *Loxl1*, *P4hb*, *Plod2*, *Serpinh1*), as well as collagens themselves (*Col1a1*, *Col1a2*, *Col3a1*, *Col4a1*, *Col5a1*, *Col5a2*, *Col6a2*, *Col8a1*, *Col11a1*, *Col14a1*, *Col15a1*, *Col18a1*) (Figure 5A). The majority of the genes within these pathways were most responsive to acute exercise between 10 and 20 days of training.

A number of other pathways showed remarkably similar responses to acute exercise between species including genes associated with translation initiation, ribosomal specialization, and large and small ribosomal subunits (*Eif4a1*, *Rpl3*, *Rp4*, *Rpl12*, *Rpl13a*, *Rpl15*, *Rpl18*, *Rpl23*, *Rpl34*, *Rplp0*, *Rps12*, *Rps15*, *Rps18*, *Rps20*, *Rpsa*, *Rps26*) (Figure 6A).[36,37] These associated genes showed patterns of expression similar to the stress response genes, peaking after just 2 days of stimulation before gradually declining (Figure 4). These early increases in ribosomal gene expression are a common feature of muscle hypertrophy, as ribosome abundance is a primary determinant of increased protein synthesis and translational capacity. We see them enhanced in both rat and mouse, but without muscle growth in the mouse.

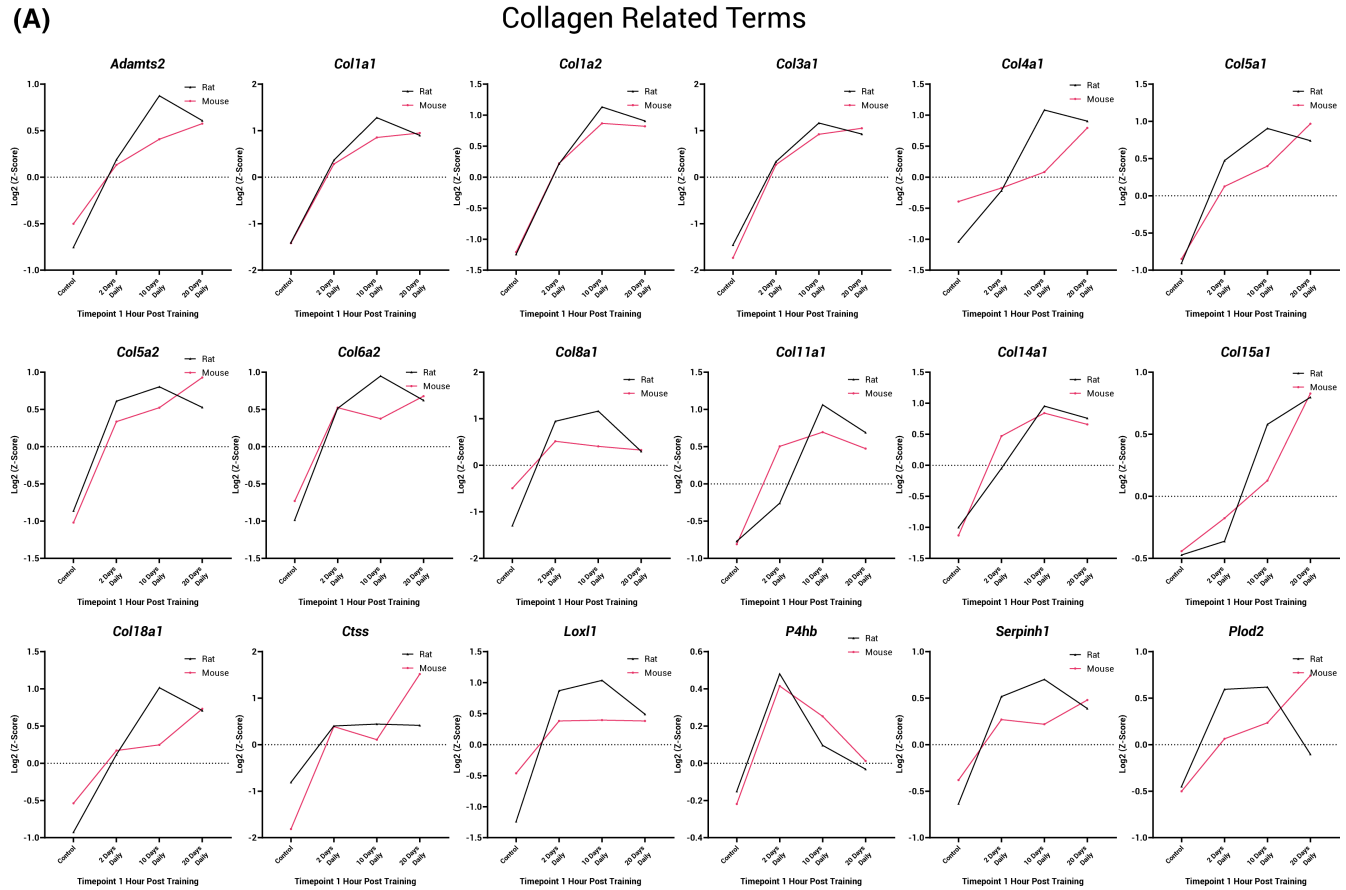

FIGURE 5 Collagen and extracellular matrix-related genes show strong similarities between species and are progressively upregulated in response to resistance exercise. (A) Log^2 *z*-scores of the Deseq2 normalized transcript abundance in control muscle and muscle after acute exercise with 2, 10, and 20 days of training history. Rat gene expression is indicated by black lines and mouse gene expression is indicated by pink lines.

Similarly, 23 genes (*Capn2*, *Ccnd1*, *Diaph1*, *Flnc*, *Fn1*, *Ilk*, *Itga5*, *Itga7*, *Lamc1*, *Lamc2*, *Mapk9*, *Myl12a*, *Mylk2*, *Parvb*, *Pdgfb*, *Pxn*, *Src*, *Thbs1*, *Thbs3*, *Tln1*, *Vcl*, *Vegfa*, *Zyx*) associated with focal adhesion followed similar patterns in rat and mouse in response to acute exercise which suggests that the stimulation provides a similar mechanical stress in both species (Figure 6B). Similar strong concordance was found in genes associated with autophagy (Figure 6C). This gene set included a number of microtubule-associated genes (*Dynll1*, *Map1lc3b*, *Tuba1a*, *Tuba1b*, *Tuba1c*, *Tuba4a*, *Tubb2b*, *Tubb4b*, *Tubb6*, *Vim*) and genes associated with mitochondrial control/mitophagy (*Pink1*, *Prkn*, *Ulk1*, *Vdac1*). Interestingly *Prkn*, an E3 ligase involved in the removal of damaged mitochondria, was the only gene within this group to show discordance being significantly upregulated in the mouse after 2-days but significantly downregulated in the rat before converging to similar levels after 10 and 20 days of exercise. Further similarities between species were observed for pathways broadly associated with "glucose/glycogen metabolism" including 10 genes encoding important proteins involved in glucose transport, glycogenolysis, and glycogen synthesis (*Agl*, *Calm1*, *Gbe1*, *Hk2*, *Pgm1*, *Phka1*, *Phkb*, *Phkg1*, *Pygm*, *Tbc1d1*) and 12 genes associated with "TGF-beta signaling" (*Acvr1b*, *E2f4*, *Fst*, *Id1*, *Id2*, *Ppp2ca*, *Rgma*, *Rpsk6kb1*, *Smad3*, *Tgfb1*, *Tgif1*, *Thbs1*). Individual plots for these genes, and genes in Figure 6A–C are presented in Figures S1–S5.

3.4 | Identification of divergent transcriptional responses between species to progressive resistance exercise

Although, we identified a large number of genes showing similar responses to acute exercise in rat and mouse during a period of daily training, most DEGs were species-specific in that they appeared as a DEG in one species but not the other (Figure 3A,D,G). However, we further filtered the species-specific DEGs identified in this analysis by assessing Pearson's correlations between the mouse and rat log^2 fold changes in gene expression in response to acute exercise. Many genes had similar directionality

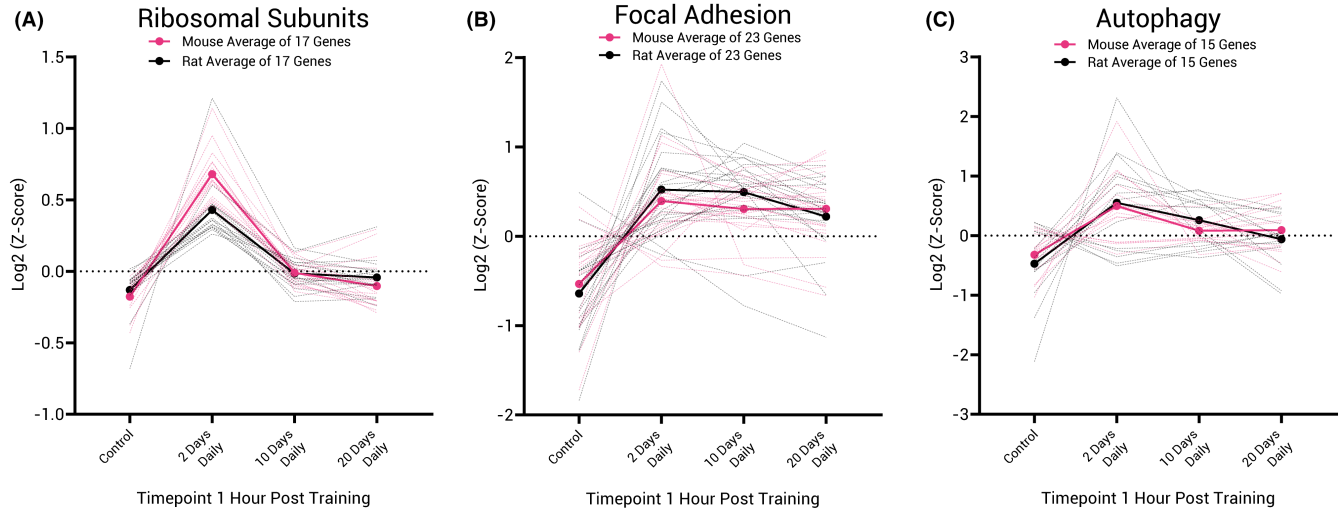

FIGURE 6 Strong concordance between species in gene expression related to ribosomal subunits, focal adhesion, and autophagy in response to resistance exercise. Log^2 *z*-scores of the Deseq2 normalized transcript abundance in control muscle and muscle after acute exercise with 2, 10, and 20 days of training. (A) Mean and individual gene traces for 17 genes associated with "Ribosomal Subunits." (B) Mean and individual gene traces for 23 genes associated with "Focal Adhesion." (C) Mean and individual gene traces for 15 genes associated with the term "Autophagy." The mean Log^2 *z*-score for the rat acute exercise responses is indicated by a solid black line and the mean Log^2 *z*-score for the mouse acute exercise responses is indicated by a solid pink line. Individual rat gene responses are indicated by dashed black lines and individual mouse gene responses are indicated by dashed pink lines.

of fold change in both species, despite not reaching the FDR cut off of 5% in one of the species. Across all training timepoints, between 68.5% and 78.7% of DEGs showed similar directionality, suggesting that a large proportion of the transcriptional response to acute exercise is conserved between mice and rats, yet it may differ in amplitude of response which results in missing an FDR cut-off of 5%. On the other hand, between 21.3% and 31.5% of genes identified through this analysis were oppositely regulated between species (indicated by red circles in Figure 7A,C,E).

In the 2-day acute exercise response (Figure 7A), 74.7% of the rat 2-day DEGs showed similar directionality in the mouse and 72.5% of the mouse 2-day DEGs showed similar directionality in the rat, despite not reaching significance in one species; 25.3% and 27.5% of rat and mouse DEGs respectively were oppositely regulated. In the 10-day acute exercise response (Figure 7C), 73.9% of the rat 10-day DEGs showed similar directionality in the mouse and 68.5% of the mouse 10-day DEGs showed similar directionality in the rat; 26.1% and 31.5% of rat and mouse DEGs respectively were oppositely regulated. Similarly in the 20-day acute exercise response (Figure 7E), 78.7% of the rat 20-day response DEGs showed similar directionality in the mouse and 78.4% of the 20-day mouse DEGs showed similar directionality in the rat; 21.3% and 21.6% showed opposing changes in gene expression in the 20-day acute exercise response comparison.

To examine further the biological processes represented by the oppositely regulated genes, we performed analysis to reveal enriched pathways (Figure 7B,D,F). Interestingly, while there were transient changes in the enrichment of DEGs common to both species, the pathways enriched at 2, 10, and 20 days showed strong evidence for differences in metabolic processing in response to electrical stimulation between species. This included 106, 97, and 60 genes associated with "Metabolic Pathways" after 2, 10, and 20 days of daily training respectively. In total, 13 of these genes were associated with "Carbon metabolism" (*Acads*, *Acss2*, *Cat*, *Dlst*, *Esd*, *Gcsh*, *Gpt*, *Hibch*, *Mcee*, *Mdh1*, *Mdh2*, *Pdhb*, *Tkt*) (Figure 8A). A number of these genes are associated with the mitochondrion to provide substrate for the tricarboxylic acid cycle or to produce/convert substrates to tricarboxylic acid cycle intermediates – cleavage of glycine for degradation, production of pyruvate, and glutamate, conversion of malate to oxaloacetate and facilitating the conversion of pyruvate to acetyl-coA. These components are upregulated in the mouse in the acute response to exercise after 2 and 10 days of training but are downregulated in the rat at the same timepoints suggesting that the metabolic demand of the identical activity pattern may be different in rat and mouse tibialis anterior muscle. Furthermore, we identified 21 genes associated with "mitochondrial translation" (*Eif3k*, *Eif4a2*, *Eif5*, *Mrpl3*, *Mrpl4*, *Mrpl5*, *Mrpl6*, *Mrpl40*, *Mrpl41*, *Mrpl42*, *Mrpl44*, *Mrpl45*, *Mrpl51*, *Mrps5*, *Mrps14*, *Mrps15*, *Mrps21*, *Mtrf1l*, *Pabpc1*, *Rpl5*, *Srp72*), including genes involved in ribosome recruitment and translation initiation, large and small mitochondrial ribosomal protein complexes, and mitochondrial translation termination

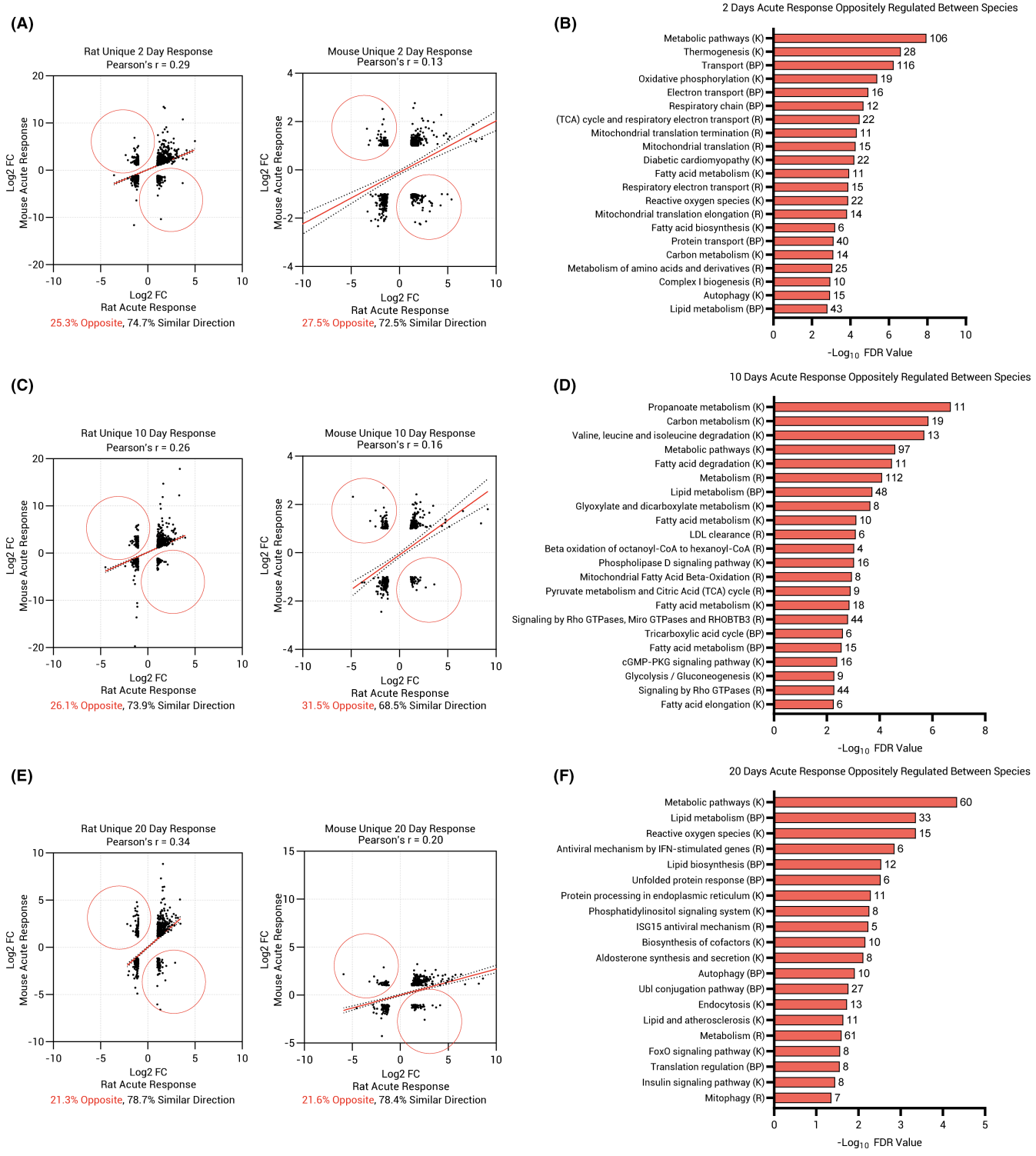

FIGURE 7 Species-specific acute transcriptional responses to resistance exercise in rats and mice. (A) Genes identified to be differentially expressed (FDR = 5%) in response to acute exercise (2-day response) in only 1 species (Figure 3A) plotted as Pearson's correlations. (B) Pathway analysis of oppositely regulated genes (red circles) identified in the day 2 acute exercise response. (C) Genes identified to be differentially expressed (FDR = 5%) in response to acute exercise (10-day response) in only 1 species (Figure 3D) plotted as Pearson's correlations. (D) Pathway analysis of oppositely regulated genes (red circles) identified in the day 10 acute exercise response. (E) Genes identified to be differentially expressed (FDR = 5%) in response to acute exercise (20-day response) in only 1 species (Figure 3A) plotted as Pearson's correlations. (F) Pathway analysis of oppositely regulated genes (red circles) identified in the day 20 acute exercise response. Pathways and their associated databases are annotated as follows: KEGG pathway (K), reactome pathway (R), and GO biological process (BP). The number of genes associated with each pathway is presented adjacent to each pathway. Data for Figure 7A–F are available in Data S2.

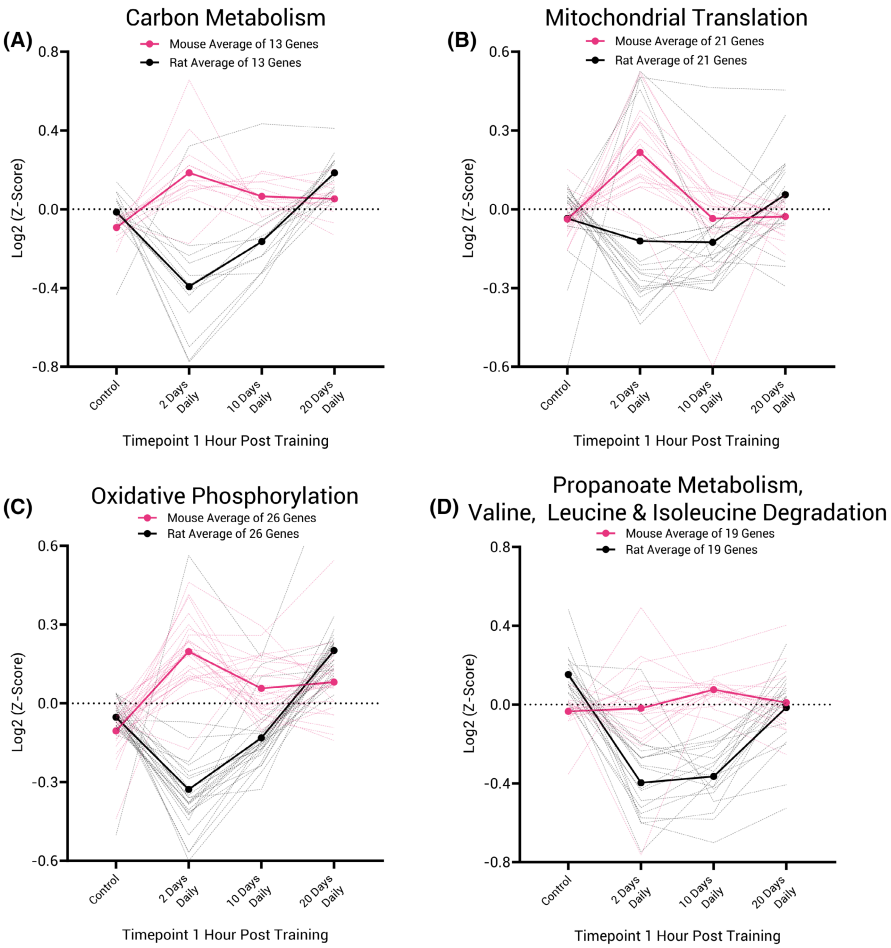

FIGURE 8 Metabolic pathways and mitochondrial translation are oppositely regulated between rat and mouse in response to acute resistance exercise. Log^2 *z*-scores of the Deseq2 normalized transcript abundance in control muscle and muscle after acute exercise with 2, 10, and 20 days of training history. (A) Mean and individual gene traces for 13 genes associated with "carbon metabolism." (B) Mean and individual gene traces for 21 genes associated with "mitochondrial translation." (C) Mean and individual gene traces for 26 genes associated with the term "oxidative phosphorylation." (D) Mean and individual gene traces for 19 genes associated with the term "propanoate metabolism, valine, leucine and isoleucine degradation." The mean Log^2 *z*-score for the rat acute exercise responses is indicated by a solid black line and the mean Log^2 *z*-score for the mouse acute exercise responses is indicated by a solid pink line. Individual rat gene responses are indicated by dashed black lines and individual mouse gene responses are indicated by dashed pink lines.

protein, (Figure 8B). Furthermore, as well as the protein synthetic machinery required to produce mitochondria, we also found discordance between species in 26 genes associated with "oxidative phosphorylation" (*Atp5pb*, *Atp6v1a*, *Atp6v1e1*, *Cox5b*, *Cox7b*, *Dlst*, *Etfb*, *Gstz1*, *Hagh*, *Mdh2*, *Ndufa4*, *Ndufa8*, *Ndufb3*, *Ndufb4*, *Ndufb5*, *Ndufb6*, *Ndufc2*, *Ndufs3*, *Ndufs4*, *Ndufs6*, *Ndufv3*, *Pdhb*, *Ppa2*, *Sdhd*, *Surf1*, *Uqcr10*). This gene set included a number of mitochondrial complex-associated genes, (Figure 8C). Again, this family of genes is upregulated in the mouse after 2-days of exercise, whereas it is consistently downregulated at all timepoints in the rat until 20 days when it is upregulated. As previously reported, the plateau in hypertrophy in the rat occurs after around 20 days when the muscle shifts to a more oxidative phenotype in response to Spillover resistance training. The observation that the mouse transcriptome seems to make this response immediately in response to resistance exercise training suggests that the mouse prioritizes energy availability, in contrast to the rat which seems to prioritize muscle growth before a later shift to more oxidative metabolism. We can hypothesize that the exercise session produces a more profound energy deficit in the mouse TA than in the rat, and this hypothesis can be tested in future experiments.

A similar discordance between species was found in 19 genes associated with "propanoate metabolism and valine, leucine and isoleucine degradation" (*Aacs*, *Acaa2*, *Acads*, *Acss1*, *Aldh2*, *Aldh9a1*, *Bckdha*, *Echdc1*, *Echs1*, *Hadh*, *Hadha*, *Hadhb*, *Hibadh*, *Ldha*, *Ldhb*, *Mccc1*, *Pccb*, *Sucla2*, *Suclg1*), (Figure 8D). A number of these genes are involved in the regulation of energy metabolism and

are again downregulated in the rat but remain either unchanged or partially upregulated in the mouse. Individual gene plots for Figure 8A–D are available in Figures S6–S9. Further discordant pathways included "fatty acid/lipid metabolism, degradation, and biosynthesis," "reactive oxygen species," "phosphatidylinositol signaling," "insulin-related terms," "foxo signaling," as well as a number of pathways involved in "translation regulation," "ubiquitin-like protein conjugation," and the "unfolded protein response." The genes included in these pathways are listed in Data S1.

3.5 | Markers of muscle denervation, muscle atrophy, and myogenesis

We also chose to probe genes associated with various paradigms of muscle loss. Specifically, we investigated genes commonly associated with the ubiquitin–proteasome system, genes associated with various forms of muscle atrophy and well-known markers of disuse caused by denervation or nerve silencing previously reported by our group and others.[38–41] Despite no histological evidence of denervation in the mouse, we sought to investigate any transcriptional changes that may infer that the muscle is programmed not to grow, despite a large number of anabolic gene signatures (Figure 3). While we recognize that changes in gene expression do not infer protein level or activity, we identified in the mouse tibialis anterior a large increase in the mRNA abundance of 11 of the 17 genes that encode alpha and beta proteasomal subunits of the 20s proteasome complex, all of which contribute to its assembly as a complex to remove protein substrates that are damaged or no longer needed, (Figure 9A). Most of these genes (*Psma1*, *Psma2*, *Psma4*, *Psma6*, *Psma7*, *Psmb1*, *Psmb3*, *Psmb4*, *Psmb5*, *Psmb5*, *Psmb6*) are unresponsive or downregulated in response to an acute training stimulus in the rat but are all substantially upregulated in the mouse in the 2-day acute response. Similar patterns are observed for the ATPase and non-ATPase subunits of the 19s proteasome and activator/inhibitor complexes, (Figure 9B,C). Genes encoding proteasome assembly chaperones are also upregulated in the mouse, but are seemingly unresponsive in the rat, (Figure 9D). Again, while this does not infer proteasomal activity, transcribing genes costs energy so it is indicative of the need for greater degradation of proteins following exercise, or a greater need for 26s proteasome complexes to be available within the muscle fiber. The fact that this substantial increase is not found or is reduced in amplitude in the rat perhaps indicates how a robust hypertrophy is possible in response to electrical nerve stimulation.

We also studied the timecourse of gene expression of a number of genes associated with muscle atrophy, denervation, and nerve silencing. As depicted in Figure 9E,F, we show that a number of these marker genes (*Mstn*, *Fbxo32*, *Trim63*, *Chrnd*, *Musk*, *Ncam1*, *Hdac4*, *Myog*) are upregulated in the mouse, and in this case, the same temporal patterns of change are observed in the rat. As the muscle grows in the rat, it is hard to postulate that this signature is indicative of denervation in the mouse when the same electrical stimulation pattern is provided in both species. We note that the majority of these genes that have been reported to change with denervation are also acutely altered in the hours post-exercise to regulate rates of protein synthesis and degradation. As our samples are taken 1-h post-exercise, further sampling of the basal transcriptome at each trained state prior to exercise will be important for future interpretations. Despite this, our histological analysis shows that the mouse muscles are healthy and the lack of growth following our training paradigm is most likely attributable to a net negative protein balance.

Expression of the myogenic genes, whose behavior is closely correlated with the determination and differentiation of precursor cells into mature skeletal muscle cells, was remarkably similar in rat and mouse, Figure S10A. For *Pax7* and *Mymx* (Myomixer), a biphasic response was observed in both species. This supports our hypothesis that a growth response was activated in the mouse muscles, but failed to produce actual increases in mass, presumably because of some downstream limitation. We also performed single cell deconvolution using CIBERSORTx, a digital cytometry approach for bulk RNA sequencing[33,34] to detect the relative percent of cell fractions influencing the tissue transcriptome, Figure S10B–D. Imputed cell fractions were suggestive of slightly different cell responses between species which included larger Dpp4+ fibroadipogenic cell influence in the exercised mouse muscles, but greater Osr1+ fibroadipogenic cells in exercised rat muscles, Figure S10D. Interestingly, the muscle stem cell response was also significantly greater in the rat-exercised muscles than the mouse-exercised muscles, $p < .0001$.

4 | DISCUSSION

In this investigation, we identified concordance and discordance in the acute transcriptional responses between mice and rats to identical nerve stimulation parameters in free-living conditions. Skeletal muscle phenotyping over a timecourse of response to resistance exercise training revealed a progressive hypertrophy in the rat muscle, but the same stimulus had little effect on the mouse in

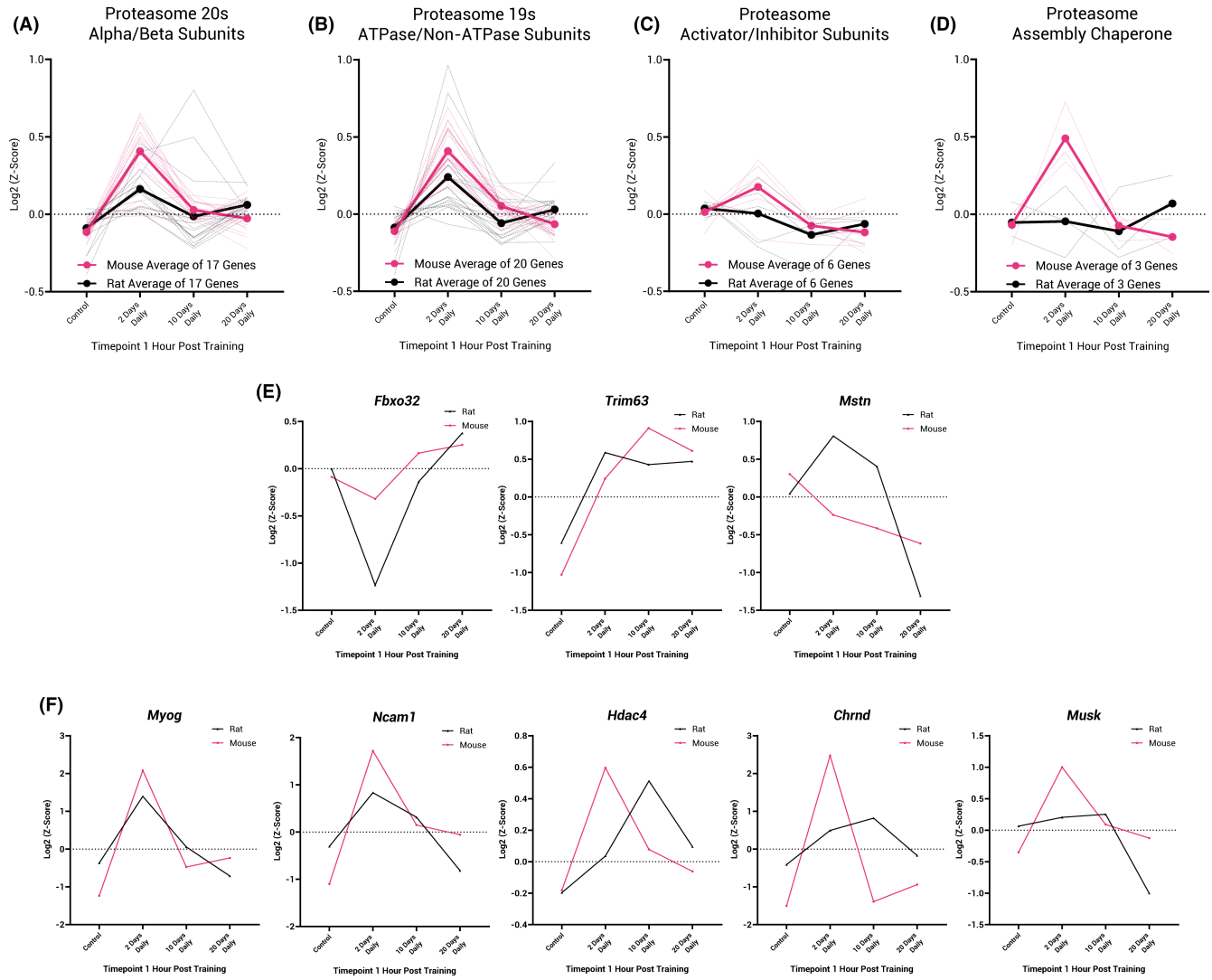

FIGURE 9 Greater increases in 26s proteasome and proteasome assembly chaperone gene expression in mice compared with rats may inhibit the early hypertrophic response. Log^2 *z*-scores of the Deseq2 normalized transcript abundance in control muscle and muscle after acute exercise with 2, 10, and 20 days of training. (A) Mean and individual gene traces for 17 genes associated with Alpha/Beta subunits of the 20s proteasome. (B) Mean and individual gene traces for 20 genes associated with "ATPase and non-ATPase subunits of the 19s proteasome." (C) Mean and individual gene traces for 6 genes associated with "proteasome activator/inhibitor complexes." (D) Mean and individual gene traces for 3 genes associated with "proteasome assembly chaperones." The mean Log^2 *z*-score for the rat acute exercise responses is indicated by a solid black line and the mean Log^2 *z*-score for the mouse acute exercise responses is indicated by a solid pink line. Individual rat gene responses are indicated by dashed black lines and individual mouse gene responses are indicated by dashed pink lines. (E) Common atrophy associated genes and (F) genes associated with denervation. Rat gene expression is indicated by black lines and mouse gene expression is indicated by pink lines.

terms of growth. We asked the question, did the mouse not mount a response to the exercise, or was the stimulus somehow ineffective in that species? No, in both species the stimulation generated visible contractions and the transcriptional response was complex and substantial with many common features but also striking differences. Combining the timecourse assessments with RNA sequencing of the acute exercise response after 2, 10, and 20 training sessions, we found that there are large commonalities between the acute transcriptional response to exercise in mouse and rat tibialis anterior muscle across the timecourse of adaptation including stress responses, focal adhesion, collagen homeostasis, ribosomal biogenesis, and autophagy. However, we were able to identify species-specific unique transcriptional responses mainly relating to metabolic processes, energy homeostasis and mitochondrial biogenesis, and these are therefore most probably related to the discordant growth response.

We identified remarkable concordance between both stress response and mechanical stress-associated genes which is indicative that the contractile stimulus and the response to that stimulus are extremely similar between

species. However, our data demonstrates that the appearance of some components of the transcriptional exercise response typically associated with muscle hypertrophy (immediate-early genes and ribosomal biogenesis), cannot be taken as sufficient evidence that subsequent hypertrophy will take place with repeated exercise of the same type, (Figures 3–6). Despite concordance in the mRNA level of key transcriptional regulators between species and with training status (*Ankrd1*, *Atf3*, *Csrnp1*, *Egr1*, *Fos*, *Hif1a*, *Jun*, *Junb*, *Jund*, *Myc*, *Nfatc3*, *Ppargc1a*, *Nr4a1*, *Nr4a2*, *Nr4a3*, *Hspa1a*, *Hspa1b*, *Hspb1*, *Hspb2*, *Hspb6*, *Hspb7*, *Hspb8*), further work should elucidate whether their activity is conserved between species. The strong concordance in collagen and collagen homeostasis-related genes also suggests that the muscle undergoes similar structural remodeling in response to stimulation, yet a hypertrophic response is lacking.

We propose that one contribution to the lack of muscle hypertrophy in the mouse in response to programmed electrical stimulation occurs as a result of different metabolic requirements of the exercise bout which results in a different transcriptional response. We highlight that a major difference between these species is that although genes involved in glucose and glycogen metabolism, including transporters and rate-limiting enzymes, show a concordant response in response to exercise, genes involved in carbon metabolism and leucine, isoleucine, and valine degradation are suppressed in the early response to acute exercise in the rat, but upregulated in the mouse. This may suggest that the mouse has an increased demand for anaplerotic substrates post-exercise that are supplied through increased amino acid metabolism. This increased demand for free amino acids in muscle to replenish the citric acid cycle substrates may increase protein degradation in the mouse which precludes a growth response. We have not measured protein synthesis and degradation rates or net balance, but such measurements would prove informative in understanding the lack of hypertrophy. However, a number of papers have used similar paradigms, stimulating the entire sciatic nerve to elicit resisted high-force contractions of the lower leg muscles.[23,42] These studies have shown that electrical stimulation can invoke an increase in protein synthesis in the hours following cessation of contraction. This has also been shown to be concomitant with the rapamycin-sensitive element of mTOR which signals to increase phosphorylation of several residues on P70 and S6 proteins.[43] Electrical stimulation is clearly capable of inducing a protein synthetic response and for growth, this is often accompanied by a reduction in 20S proteasome activity. For example, following synergist ablation in mice, it has been recorded that 20S proteasome activity is reduced by ~63% in the plantaris, and ~20% in the soleus, resulting in a greater rate and magnitude of growth in the plantaris.[44] By contrast, our gene expression data infers an increased requirement for the 20S proteasome system (Figure 9) in the mouse after a resistance training bout. Again, we propose that the lack of growth following our training paradigm in the mouse is most likely attributable to a net negative protein balance but will require confirmation.

Alongside the discordance in the genes associated with carbon metabolism and amino acid availability, the mouse transcriptome showed upregulation of a large network of genes involved in lipid oxidation, as well as genes encoding subunit constituents of all 5 mitochondrial complexes and proteins involved in their appropriate assembly. Genes encoding members of the pyruvate dehydrogenase complex, TCA cycle intermediate enzymes, oxidative metabolism, and genes encoding proteins important for mitochondrial translation initiation and capacity were also upregulated. These are oppositely regulated in the rat, until 20 days of training when muscle hypertrophy has ceased. We did not directly test substrate availability, usage or metabolic enzyme activity/content after acute exercise in our model, but it is possible that the mouse tibialis anterior being less oxidative than the rat and rabbit tibialis anterior muscle[45] promotes an upregulation of metabolic components even during or following our "typical" resistance training protocol of 5 sets of 10 repetitions which may not be required to maintain homeostasis after stimulation with the same protocol in the rat.

Since our publication of the timecourse of change in the *acute* transcriptional responses to exercise over 4 weeks of daily training in the rat, there have been very few additional studies that investigate this important aspect of the exercise response. Furrer et al. reported from a study of endurance training in mice that while the basal (rested) transcriptomes of trained and untrained muscles are remarkably similar, training status substantially affects the acute transcriptional response to exercise[17] including increases and decreases in the amplitude of gene expression as well as changing the phase or rate of response post-exercise (peaking earlier post-exercise).[46] Training status was also reported to change the transcriptional program itself with the loss of response in some genes and production of de novo responses of other genes as training status increases, similar to our report. To date, similar investigations into the modulation of transcription by training status have been limited to endurance or high-intensity interval exercise responses,[47,48] and our new data and previous data from our group[17] remain a valuable resource for understanding training status modulation of the acute transcriptional response to resistance-like exercise. Whether the mouse is a suitable model to study human muscle growth or wasting is an important and current research question. A recent transcriptomic survey of

4 muscles in mice and rats across the lifespan, suggests that rats mimic human aging and sarcopenia more closely than mouse.[38] Large differences in the progressive dysregulation of genes associated with metabolic processes and mitochondrial function were found in rat, but not in mouse suggesting that the use of the mouse or mouse tissue must be carefully interpreted when translating to aspects of human aging and sarcopenia. We propose that the lack of growth in the mouse in response to a daily session of electrical stimulation, which causes hypertrophy in rats and in humans[49–51] suggests that work in the mouse needs careful interpretation when applied to human hypertrophy or for example, optimization of neuromuscular electrical stimulation interventions for clinical use in humans.

We identify a number of limitations and future considerations within these experiments including the limited timepoints post-exercise. We use 1-h post exercise as it has previously been identified as the timepoint which yields the largest transcriptional changes in skeletal muscle,[52] but we cannot discount the possibility of different transcriptional responses occurring in different phases post-exercise between species as recently reported.[46] We also understand that transcriptional regulation of mRNAs is one aspect of the adaptive response to exercise and accompanying protein and metabolomic data will help future understanding of what drives the transcriptional response and resultant changes in muscle size.

Overall, our findings illustrate that there are both concordant and discordant elements in the acute responses to exercise in the same muscle in two very closely related murine species. The exercise response is not uniform across species, despite using highly controlled, programmed exercise in free-living animals, and differs with different stages of training. Further study of epigenetic control, transcription factor kinetics and post-transcriptional regulation of mRNAs will help to explain the hierarchy of the response illustrated in this study in which adaptation of the metabolic support for contraction in the mouse appears to be triggered before the net increase in protein generation that is required for muscle growth.

AUTHOR CONTRIBUTIONS

Mark R. Viggars, Hazel Sutherland, and Jonathan C. Jarvis designed experiments. Jonathan C. Jarvis and Christopher P. Cardozo secured funding and statutory permissions. Mark R. Viggars, Hazel Sutherland, and Jonathan C. Jarvis performed experiments. Mark R. Viggars and Jonathan C. Jarvis analyzed the data and contributed to interpretations. Mark R. Viggars and Jonathan C. Jarvis wrote the manuscript with assistance from all authors. All authors contributed to the research of the published work and have read and approved the final manuscript.

ACKNOWLEDGMENTS

We acknowledge the staff of the Life Sciences Support Unit at LJMU for their expert husbandry. We acknowledge the support of The Competence Team Implanted Devices at the Medical University of Vienna for their continued support in the design and supply of implanted stimulators.

DISCLOSURES

The authors declare no conflicts of interest.

DATA AVAILABILITY STATEMENT

The data that support the findings of this study are openly available via the National Institutes of Health Gene Expression Omnibus. Raw RNA sequencing data (FASTq) is available through GEO Accessions, GSE196147 and GSE228050. Processed, normalized count data for RNA sequencing experiments are available in Data S1. Any additional data are available upon request from the corresponding author.

ORCID

Mark R. Viggars https://orcid.org/0000-0002-0722-7051
Hazel Sutherland https://orcid.org/0000-0002-5570-1379
Christopher P. Cardozo https://orcid.org/0000-0003-4013-2537
Jonathan C. Jarvis https://orcid.org/0000-0001-8982-6279

REFERENCES

1. Gale CR, Martyn CN, Cooper C, Sayer AA. Grip strength, body composition, and mortality. *Int J Epidemiol*. 2007;36(1):228-235.
2. Newman AB, Kupelian V, Visser M, et al. Strength, but not muscle mass, is associated with mortality in the health, aging and body composition study cohort. *J Gerontol A Biol Sci Med Sci*. 2006;61(1):72-77.
3. Corcos DM, Robichaud JA, David FJ, et al. A two-year randomized controlled trial of progressive resistance exercise for Parkinson's disease. *Mov Disord*. 2013;28(9):1230-1240.
4. Hashida R, Kawaguchi T, Bekki M, et al. Aerobic vs. resistance exercise in non-alcoholic fatty liver disease: a systematic review. *J Hepatol*. 2017;66(1):142-152.
5. Mcleod JC, Stokes T, Phillips SM. Resistance exercise training as a primary countermeasure to age-related chronic disease. *Front Physiol*. 2019;10:645.
6. Braith RW, Stewart KJ. Resistance exercise training: its role in the prevention of cardiovascular disease. *Circulation*. 2006;113(22):2642-2650.
7. Bodine SC, Stitt TN, Gonzalez M, et al. Akt/mTOR pathway is a crucial regulator of skeletal muscle hypertrophy and can prevent muscle atrophy in vivo. *Nat Cell Biol*. 2001;3(11):1014-1019.
8. Glass DJ. Skeletal muscle hypertrophy and atrophy signaling pathways. *Int J Biochem Cell Biol*. 2005;37(10):1974-1984.
9. Ogasawara R, Fujita S, Hornberger TA, et al. The role of mTOR signalling in the regulation of skeletal muscle mass in a rodent model of resistance exercise. *Sci Rep*. 2016;6(1):31142.

10. Ogasawara R, Arihara Y, Takegaki J, Nakazato K, Ishii N. Relationship between exercise volume and muscle protein synthesis in a rat model of resistance exercise. *J Appl Physiol*. 2017;123(4):710-716.
11. Steinert ND, Potts GK, Wilson GM, et al. Mapping of the contraction-induced phosphoproteome identifies TRIM28 as a significant regulator of skeletal muscle size and function. *Cell Rep*. 2021;34(9):108796.
12. Smith GR, Zhao B, Lindholm ME, et al. Multiomic identification of key transcriptional regulatory programs during endurance exercise training. bioRxiv 2023.
13. McCarthy JJ, Srikuea R, Kirby TJ, Peterson CA, Esser KA. Inducible Cre transgenic mouse strain for skeletal muscle-specific gene targeting. *Skelet Muscle*. 2012;2:8.
14. Murach KA, McCarthy JJ, Peterson CA, Dungan CM. Making mice mighty: recent advances in translational models of load-induced muscle hypertrophy. *J Appl Physiol*. 2020;129(3):516-521.
15. Baar K, Esser K. Phosphorylation of p70(S6k) correlates with increased skeletal muscle mass following resistance exercise. *Am J Physiol*. 1999;276(1):C120-C127. doi:10.1152/ajpcell.1999.276.1.C120
16. Nader GA, Esser KA. Intracellular signaling specificity in skeletal muscle in response to different modes of exercise. *J Appl Physiol*. 2001;90(5):1936-1942.
17. Viggars MR, Sutherland H, Lanmüller H, Schmoll M, Bijak M, Jarvis JC. Adaptation of the transcriptional response to resistance exercise over 4 weeks of daily training. *FASEB J*. 2022;37(1):e22686.
18. Schmoll M, Unger E, Sutherland H, et al. SpillOver stimulation: a novel hypertrophy model using co-contraction of the plantar-flexors to load the tibial anterior muscle in rats. *PloS One*. 2018;13(11):e0207886. doi:10.1371/journal.pone.0207886
19. Viggars MR, Wen Y, Peterson CA, Jarvis JC. Automated cross-sectional analysis of trained, severely atrophied and recovering rat skeletal muscles using MyoVision 2.0. *J Appl Physiol*. 2022;132:593-610.
20. Hardee JP, Mangum JE, Gao S, et al. Eccentric contraction-induced myofiber growth in tumor-bearing mice. *J Appl Physiol*. 2016;120(1):29-37.
21. Sato S, Gao S, Puppa MJ, Kostek MC, Wilson LB, Carson JA. High-frequency stimulation on skeletal muscle maintenance in female cachectic mice. *Med Sci Sports Exerc*. 2019;51(9):1828-1837.
22. Lotri-Koffi A, Pauly M, Lemarié E, et al. Chronic neuromuscular electrical stimulation improves muscle mass and insulin sensitivity in a mouse model. *Sci Rep*. 2019;9(1):7252.
23. You J-S, McNally RM, Jacobs BL, et al. The role of raptor in the mechanical load-induced regulation of mTOR signaling, protein synthesis, and skeletal muscle hypertrophy. *FASEB J*. 2019;33(3):4021-4034.
24. Potts GK, McNally RM, Blanco R, et al. A map of the phosphoproteomic alterations that occur after a bout of maximal-intensity contractions. *J Physiol*. 2017;595(15):5209-5226.
25. Viggars MR, Owens DJ, Stewart C, Coirault C, Mackey AL, Jarvis JC. PCM1 labeling reveals myonuclear and nuclear dynamics in skeletal muscle across species. *Am J Physiol Cell Physiol*. 2023;324(1):C85-C97.
26. Owens DJ, Messéant J, Moog S, et al. Lamin-related congenital muscular dystrophy alters mechanical signaling and skeletal muscle growth. *Int J Mol Sci*. 2021;22(1):306.
27. Hughes DC, Turner DC, Baehr LM, et al. Knockdown of the E3 ubiquitin ligase UBR5 and its role in skeletal muscle anabolism. *Am J Physiol Cell Physiol*. 2021;320(1):C45-C56.
28. Dobin A, Davis CA, Schlesinger F, et al. STAR: ultrafast universal RNA-seq aligner. *Bioinformatics*. 2013;29(1):15-21.
29. de Jong TV, Chen H, Brashear WA, et al. mRatBN7. 2: familiar and unfamiliar features of a new rat genome reference assembly. *Physiol Genomics*. 2022;54(7):251-260.
30. Howe K, Dwinell M, Shimoyama M, et al. The genome sequence of the Norway rat, *Rattus norvegicus* Berkenhout 1769. *Wellcome Open Res*. 2021;6(118):118.
31. Love MI, Huber W, Anders S. Moderated estimation of fold change and dispersion for RNA-seq data with DESeq2. *Genome Biol*. 2014;15(12):550.
32. Dennis G, Sherman BT, Hosack DA, et al. DAVID: database for annotation, visualization, and integrated discovery. *Genome Biol*. 2003;4(9):P3.
33. Newman AM, Steen CB, Liu CL, et al. Determining cell type abundance and expression from bulk tissues with digital cytometry. *Nat Biotechnol*. 2019;37(7):773-782.
34. Murach KA, Liu Z, Jude B, et al. Multi-transcriptome analysis following an acute skeletal muscle growth stimulus yields tools for discerning global and MYC regulatory networks. *J Biol Chem*. 2022;298(11):102515.
35. Ashida Y, Himori K, Tatebayashi D, Yamada R, Ogasawara R, Yamada T. Effects of contraction mode and stimulation frequency on electrical stimulation-induced skeletal muscle hypertrophy. *J Appl Physiol*. 2018;124(2):341-348.
36. Chaillou T. Ribosome specialization and its potential role in the control of protein translation and skeletal muscle size. *J Appl Physiol*. 2019;127:599-607.
37. Chaillou T, Zhang X, McCarthy JJ. Expression of muscle-specific ribosomal protein L3-like impairs myotube growth. *J Cell Physiol*. 2016;231(9):1894-1902. doi:10.1002/jcp.25294
38. Shavlakadze T, Xiong K, Mishra S, et al. Age-related gene expression signatures from limb skeletal muscles and the diaphragm in mice and rats reveal common and species-specific changes. *Skel Muscle*. 2023;13(1):11. doi:10.1186/s13395-023-00321-3
39. Fisher AG, Seaborne RA, Hughes TM, et al. Transcriptomic and epigenetic regulation of disuse atrophy and the return to activity in skeletal muscle. *FASEB J*. 2017;31(12):5268-5282.
40. Murton A, Constantin D, Greenhaff P. The involvement of the ubiquitin proteasome system in human skeletal muscle remodelling and atrophy. *Biochim Biophys Acta*. 2008;1782(12):730-743.
41. Bodine SC, Baehr LM. Skeletal muscle atrophy and the E3 ubiquitin ligases MuRF1 and MAFbx/atrogin-1. *Am J Physiol Endocrinol Metab*. 2014;307(6):E469-E484.
42. You J-S, Anderson GB, Dooley MS, Hornberger TA. The role of mTOR signaling in the regulation of protein synthesis and muscle mass during immobilization in mice. *Dis Model Mech*. 2015;8(9):1059-1069. doi:10.1242/dmm.019414
43. Tsai S, Sitzmann JM, Dastidar SG, et al. Muscle-specific 4E-BP1 signaling activation improves metabolic parameters during aging and obesity. *J Clin Invest*. 2015;125(8):2952-2964.
44. Roberts MD, Mobley CB, Vann CG, et al. Synergist ablation-induced hypertrophy occurs more rapidly in the plantaris than soleus muscle in rats due to different molecular mechanisms. *Am J Physiol Regul Integr Comp Physiol*. 2020;318(2):R360-R368.

45. Simoneau J-A, Pette D. Species-specific effects of chronic nerve stimulation upon tibialis anterior muscle in mouse, rat, Guinea pig, and rabbit. *Pflugers Arch*. 1988;412:86-92.
46. Furrer R, Heim B, Schmid S, et al. Molecular control of endurance training adaptation in mouse skeletal muscle. bioRxiv 2023. doi:10.1101/2023.02.18.529055
47. Norrbom JM, Ydfors M, Lovric A, Perry CG, Rundqvist H, Rullman E. A HIF-1 signature dominates the attenuation in the human skeletal muscle transcriptional response to high-intensity interval training. *J Appl Physiol*. 2022;132(6):1448-1459.
48. Perry CG, Lally J, Holloway GP, Heigenhauser GJ, Bonen A, Spriet LL. Repeated transient mRNA bursts precede increases in transcriptional and mitochondrial proteins during training in human skeletal muscle. *J Physiol*. 2010;588(23):4795-4810.
49. Jandova T, Narici MV, Steffl M, et al. Muscle hypertrophy and architectural changes in response to eight-week neuromuscular electrical stimulation training in healthy older people. *Life*. 2020;10(9):184.
50. Barberi L, Scicchitano BM, Musaro A. Molecular and cellular mechanisms of muscle aging and sarcopenia and effects of electrical stimulation in seniors. *Eur J Transl Myol*. 2015;25(4):231-236.
51. Kern H, Hofer C, Loefler S, et al. Atrophy, ultra-structural disorders, severe atrophy and degeneration of denervated human muscle in SCI and Aging. Implications for their recovery by Functional Electrical Stimulation, updated 2017. *Neurol Res*. 2017;39(7):660-666.
52. Group MS, Amar D, Gay NR, et al. Temporal dynamics of the multi-omic response to endurance exercise training across tissues. BioRxiv 2022. doi:10.1101/2022.09.21.508770

SUPPORTING INFORMATION

Additional supporting information can be found online in the Supporting Information section at the end of this article.

How to cite this article: Viggars MR, Sutherland H, Cardozo CP, Jarvis JC. Conserved and species-specific transcriptional responses to daily programmed resistance exercise in rat and mouse. *The FASEB Journal*. 2023;37:e23299. doi:10.1096/fj.202301611R